HHS Public Access

Author manuscript

J Cogn Neurosci. Author manuscript; available in PMC 2018 March 01.

Published in final edited form as:

J Cogn Neurosci. 2018 March ; 30(3): 281–289. doi:10.1162/jocn_a_01206.

Not doomed to repeat: Enhanced mPFC tracking of errors promotes adaptive behavior during adolescence

Ethan M. McCormick[1] and **Eva H. Telzer**[*,1]

[1]Department of Psychology and Neuroscience, University of North Carolina, Chapel Hill, North Carolina, 27599

Abstract

Feedback information is one of the most powerful forces that promotes learning, providing guidance for changes to ongoing behavioral patterns. Previous examinations of feedback learning have largely relied on explicit feedback based on task performance. However, learning is not restricted to explicit feedback, and likely involves other forms of more-subtle feedback cues. One potential form of this kind of learning may involve internally-generated feedback in response to error commission. Whether this error-related response prompts neural and behavioral adaptation that overlap with, or are distinct from, those evoked by external feedback is largely unknown. In order to explore this gap, 55 adolescents completed a difficult behavioral inhibition task designed to elicit relatively high rates of error commission during an fMRI session. We examined neural adaptation following accumulating errors (i.e. internally-generated negative feedback events) at the group level, as well as the impact of individual differences in error tracking on overall task performance. Group effects show that mPFC activation tracks accumulating errors, however, reduced tracking of errors is associated with greater total false alarms. These findings suggest that increased mPFC integration of error-related feedback is beneficial for task performance, and in concert with previous findings, suggests a domain-general role for mPFC integration of negative feedback.

Keywords

adolescence; fMRI; error-monitoring; feedback learning

Introduction

Learning involves the integration of previous behavior with new information in order to either perpetuate or change behavior. During learning, performance feedback provides an important form of information to guide future behavior, and this process of feedback learning is especially important in adolescence (Somerville et al., 2010; McCormick & Telzer, 2017a). Both positive and negative feedback sensitivity have generated substantial interest during the adolescent years, with evidence suggesting that teens are more sensitive

[*]corresponding author. Eva H. Telzer, 235 E. Cameron Avenue, Chapel Hill, NC 27514, ehtelzer@unc.edu, 919-962-9720.

Author Contributions: E.M.M. and E.H.T designed and performed research; analyzed data; and wrote the paper.

The authors declare no competing financial interests.

to positive forms of feedback (e.g. Galván, 2013; see Telzer, 2016) and potentially less sensitive to negative feedback (e.g. Ernst et al., 2005; McCormick & Telzer, 2017b). Furthermore, compared with children, adolescents show an increased ability to use feedback information to guide their learning and subsequent behavior (Peters et al., 2016; McCormick & Telzer, 2017a). This increase in feedback learning during adolescent development may help teens flexibly explore and adapt to new environments (e.g. Crone & Dahl, 2012) and promote the avoidance of unfavorable behavioral patterns.

While learning is an incredibly complex process that engages broad networks throughout the cortex (e.g. Peters et al., 2014, 2016), the medial prefrontal cortex (mPFC) is a key hub for goal representations and feedback integration into ongoing behavioral decisions in adults (van Noordt & Segalowitz, 2012) and adolescents (van Duijvenvorde et al., 2014; McCormick & Telzer, 2017b), and is involved in monitoring error commission during behavioral performance (Rubia et al., 2003). The mPFC is well-positioned as an integration hub for feedback information, sharing important structural and functional connections with the anterior cingulate cortex (Supekar et al., 2010), amygdala (Phelps et al., 2004; Gee et al., 2013), and ventral striatum (Schwarz et al., 2007; van den Bos et al., 2012). Furthermore, mPFC reactivity, especially in the mid-dorsal portion of the mPFC (medial BA 8/9) located between the dorsomedial PFC and the ventromedial PFC, in response to positive (van Duijvenvorde et al., 2014) and negative (McCormick & Telzer, 2017b) feedback predicts behavioral performance in a risk-taking context, suggesting that the information integrated in the mPFC during decision-making is important for future behavior.

The majority of prior examinations of feedback learning during adolescence employ direct and explicit feedback from the task environment (e.g., van Duijvenvoorde et al., 2008; Peters et al., 2016; McCormick & Telzer, 2017b), where participants' behavior is extrinsically rewarded or punished based on their success or failure. While a reasonably simple and direct way to examine feedback-related learning, this approach may represent an over-simplified model of how feedback guides learning and behavior in real life. Explicit feedback is most certainly one part of how learning occurs; however, another is internally-generated error signaling based on the mismatch between current behavior and learned rules or goals. Previous work has shown that adolescents show performance-related activation in regions involved in feedback processing, such as striatum during successful performance (e.g., Sattherthwaite et al., 2012) and anterior cingulate during error commission (e.g., Stevens et al., 2009). However, previous work has not assessed whether these internally-generated signals prompt internal evaluation of adolescents' current strategy following error commission and lead to subsequent changes in behavior to better align with adolescents' goals. In this context, self-generated performance-related feedback can represent an important mechanism for learning, even in the absence of external cues related to performance. Despite this, we know little about the neurobiological systems that support learning from this kind of self-generated feedback information, and whether they differ from those that support more-explicit forms of feedback learning.

To address this question, we took a novel approach by examining adolescents' neural tracking of error commission during a difficult behavioral inhibition task. During an fMRI scan, adolescents completed an adaptive version of the Stop Signal Task (SST; Logan &

Cowan, 1984), which results in greater commission of behavioral inhibition failures (i.e. false alarms) by adjusting task difficulty based on participants' prior performance. As such, we were able to look at the effect of accumulating errors on adolescents' neural representation of task behavior. We implemented a unique analytical approach, by which we tested *in vivo* encoding of errors into subsequent task representations and the neural adaptation for behavioral outcomes. The SST has been successfully used in adolescents to examine the development of cognitive control and behavioral inhibition (e.g., Williams et al., 1999; Paus, 2005; Stevens et al., 2009; Mueller et al., 2010); however, it has not previously been used to examine feedback-related neural adaptation in adolescents. We tested trial-by-trial level associations between false alarm error commission at the behavioral level and neural adaptation during subsequent trials. In particular, we included a parametric regressor for each trial, which represented the total number of errors committed. Thus, with each additional error committed, the parametric regressor increased linearly. Neural effects, therefore, represent how the brain linearly tracks the accumulation of false alarms during task performance. Compared with traditional methods of modeling task behavior and neural activation, which averages across trials, this novel approach allowed us to examine within-session, trial-by-trial neural change conditional upon accumulated error commissions. Based on the idea that errors operate as a form of self-generated negative feedback, we hypothesized that the mPFC would track the neural response to accumulating errors, and greater mPFC tracking of the accumulation of errors would predict improved task performance. In order to assess the specificity of effects to error-related neural adaptation, we performed similar analyses with a parametric modulator that tracked the accumulation of successful inhibition.

Methods

Participants

Fifty-six adolescents completed an fMRI scan. Participants were recruited from the community using a variety of approaches, including flyers, recruiting from a pool of subjects, and through local schools. We screened adolescents for use of psychoactive drugs (e.g., antidepressants, ADHD medication) and for MRI contraindications. One participant was excluded due to moving out of the field of view, leaving a final sample of fifty-five adolescents (M_{age} = 13.41 years, SD = 1.11, *range* = 12.03–15.94; 29 males; 38 European-American, 8 African-American, 3 Asian-American, 1 Native-American, 1 Brazilian, and 5 multiple ethnicity). All participants' parents had graduated high school, with all but one attending at least some college, and 40% attended or graduated from graduate/professional school. Participants provided written assent, and parents provided written consent in accordance with the University of Illinois' Institutional Review Board.

Stop Signal Task

During the scan session, participants completed a version of the Stop Signal Task (SST), a well-established behavioral inhibition paradigm (e.g., Logan & Cowan, 1984; Rubia et al., 2003). Participants were presented with a sequence of arrows (e.g. "<" or ">") enclosed within a white circle (Figure 1). Participants were instructed to make a button press (i.e. "go" response) with their right or left index finger corresponding to the direction the

presented arrow was facing. However, if the enclosing circle turned red, participants were instructed to withhold the button press (i.e. “stop”). On Go trials, arrows were presented for a fixed 750 ms within the white circle and then disappeared for a jittered period of time. On Stop trials, go-stimulus arrows were presented for a variable time (Stop Signal Delay (SSD); bounded at 50 and 350 ms;) within the white circle before the enclosing circle turned red (i.e. the stop signal). The red circle remained on the screen until 750 ms had passed from the initial presentation of the arrow to equate trial length between Go and Stop trials. At the beginning of the task, the SSD was set to 150 ms. After each successful stop trial, the SSD was lengthened by 50 ms, increasing the difficulty of inhibiting the prepotent “go” response on the next Stop trial. Alternatively, unsuccessful stops (i.e. false alarms) resulted in a shortening of the SSD by 50 ms. This approach allows the task to adapt to participants’ behavior, resulting in a relatively high incidence of false alarms compared with fixed-difficulty tasks. Importantly, this adaptive design was intended to generate significant, but not excessive, numbers of FA errors such that adolescents have sufficient error rates without being overwhelmed by the difficulty of the task. Participants were instructed to try to perform the task to the best of their ability. However, participants received no instructions related to keeping track of the number of false alarms they committed, nor did the task give any indication when a false alarm or other error was committed.

The SST was presented as one block of 186 trials, composed of 124 (2/3) Go trials and 62 (1/3) Stop trials. Trials were pseudorandomly ordered such that no more than three Go trials separated Stop trials, and that no more than two Stop trials occurred in immediate succession. Because of this ordering scheme and the disproportionate amount of Go trials, relative to Stop trials, participants develop a prepotent (or habitual) response to perform a button press that they then have to inhibit during Stop trials. Trials were separated by a jittered period that was drawn from a truncated gamma distribution centered around 1s. There was no difference in jitter length between Go and Stop trials, nor was there any difference in the frequency of arrow types (e.g. “>” or “<”) between trial types.

Behavioral Modeling—Number of false alarms (i.e. unsuccessful Stop trials) was the primary metric of task success. Because of the modeling approach we took (described in fMRI data analysis), false alarms were defined as a response during any part of a Stop trial (i.e., before or after the stop signal displayed). While our primary interest was in neural tracking to accumulated FA errors, we also calculated the latency of the stop process as a metric of behavioral inhibition success. Because the stop latency is an unobserved process (Verbruggen & Logan, 2008), it must be estimated using other behavioral indices. First, we calculated the percentage of Stop trials on which each participant committed a false alarm. Next, we determined a percentile RT value from the distribution of each participants’ reaction times on Go trials. After ordering Go RT values by latency in ascending order, we determined which RT value corresponded to the percentile value equal to the percentage of false alarms committed by that participant (Thakkar et al, 2014; e.g., a participant who committed a false alarm 10% of the time would have a percentile RT value corresponding to the 10^{th} percentile of their RT values). We also calculated the average delay between the presentation of the go (i.e., the white circle) and the stop stimuli (i.e., the red circle) within a Stop trial (i.e., stop signal delay; SSD). The SSD was then subtracted from the percentile RT

value to calculate the Stop Signal Reaction Time (SSRT), which therefore represents the theoretical latency of the Stop response, or how quickly participants can inhibit the prepotent Go response. As such, greater values of SSRT are related to poorer inhibitory control. Because SSRT is calculated using data from across the entire run, it cannot be used to assess trial-by-trail changes within-task.

fMRI Data Acquisition

Imaging data were collected using a 3 Tesla Siemens Magnetom Trio MRI scanner. The SST scan consisted of T2*-weighted echoplanar images (EPI; 180 volumes; slice thickness=3 mm; 38 slices; TR=2 s; TE=25 ms; matrix=92×92; FOV=230 mm; voxel size=2.5×2.5×3 mm^3). Structural scans were also acquired, including a T1* magnetization-prepared rapid-acquisition gradient echo (MPRAGE; 192 slices; TR=1.9 s; TE=2.32 ms; FOV= 230 mm; matrix=256×256; sagittal acquisition plane; slice thickness=0.9 mm) and a T2*-weighted, matched-bandwidth (MBW), high resolution anatomical scan (38 slices; TR=4 s; TE=64 ms; FOV=230 mm; matrix=192×192; slice thickness=3 mm). MBW and EPI images were acquired at an oblique axial orientation to maximize brain coverage and reduce drop-out in orbital and temporal regions.

fMRI data preprocessing and analysis—Preprocessing steps were completed using FSL FMRIBs Software Library (FSL v6.0; https://fsl.fmrib.ox.ac.uk/fsl/). Preprocessing steps included: correction for slice-to-slice head motion using the MCFLIRT; spatial smoothing using a 6mm Gaussian kernel, full-width-at-half maximum; high-pass temporal filtering with a 128s cutoff to remove low frequency drift across the time-series; and skull stripping of all images with BET. Functional images were co-registered sequentially to the MBW and the MPRAGE using FLIRT in order to warp them into the standard stereotactic space defined by the Montreal Neurological Institute (MNI) and the International Consortium for Brain Mapping. Individual-level independent component analysis (ICA) using MELODIC combined with an automated component classifier (Tohka et al., 2008; Neyman-Pearson threshold = 0.3) was applied to remove artifact signal (e.g. motion, physiological noise).

The Stop Signal Task was modeled using an event-related design within the Statistical Parametric Mapping software package (SPM8; Wellcome Department of Cognitive Neurology, Institute of Neurology, London, UK). Each event was modeled using a fixed duration of 750 ms. Fixed-effects models were created by including a general linear model for conditions of interest: successful go trials, successful stop trials, unsuccessful go trials (i.e. misses), and unsuccessful stop trials (i.e. false alarms). Volumes containing motion in excess of 2 mm slice-to-slice were modeled in a separate regressor of no interest. All adolescents in the final sample had less than 2 mm of slice-to-slice head motion for over 95% of total volumes. Jittered inter-trial periods were not explicitly modeled and therefore served as an implicit baseline for the task conditions of interest.

In order to examine neural tracking of error commission on a trial-by-trial level, a parametric modulator (PM) was included for go, stop, and false alarm trials, and represented the accumulated number of false alarms committed by the participant before that point in the

task. PM values began at 0 for initial trials and increased linearly by 1 for each false alarm committed. As such, trials before the commission of the first false alarm error in the task were weighted as zero; then after the first false alarm trial, subsequent trials of each type were weighted as 1 until the next false alarm trial. This continued throughout the task, with each false alarm trial resulting in the linear addition of parametric weight for subsequent trials. While participants could make a number of errors during the SST, including false alarms, misses (i.e., failing to press on a go trial) or direction mismatches (e.g., pressing left on a right-facing error), we only modeled the accumulation of false alarms for our PM. We took this approach both because other types of errors were relatively rare, and because we did not want to model different combinations of error types across individuals in the PM condition. We also did not theoretically expect other types of errors to elicit the kind of salient feedback information that would prompt behavioral and neural adaptation. As such, when referring to errors subsequently, we specifically refer to those errors that involve failures of inhibitions on Stop trials (i.e., false alarms).

Examining conditions of interest as conditional on the PM allowed us to asses which neural regions show adaptation in response to accumulating errors. As a result, a positive value in the PM condition would indicate that for each error committed, a given region showed linear increases in activation, whereas a negative value would indicate linear decreases in activation following each error. A PM was not included for miss trials due to the relatively low frequency of this event type. Contrasts were computed at the individual level for all conditions of interest.

At the group level, we conducted two sets of analyses. First, we tested how the brain tracks accumulating errors during Go trials. We focused on Go trials because they constitute the time between inhibition (i.e. Stop) trials when adolescents are able to incorporate error information and potentially update behavioral strategies in order to succeed on the next inhibition trial. Second, to examine how neural tracking of errors is associated with overall performance on the task, we conducted whole-brain regression analyses in which we regressed the total number of errors on the parametric modulation of the Go contrast. This approach allowed us to examine regions where tracking differed between those who committed high versus low levels of false alarms. Because each participants' number of false alarm errors is inextricably linked with the number of trials used to specify both the Stop and FA conditions, we restricted our analyses to the trials in the Go condition, which are independent of inhibitory success. Combining these approaches not only allows us to examine general processes of neural adaptation to error-related feedback, but also how tracking might differ between individuals who were more or less successful in their task performance. This analysis plan provides a powerful way to examine group and individual-level processes that contribute to neural adaptation and learning in the context of error commission during a cognitive control task.

Random effects, group-level analyses were run for all contrasts using GLMFlex (http://mrtools.mgh.harvard.edu/index.php/GLM_Flex). GLMFlex offers several advantages, including removing outliers and sudden activation changes in brain, corrects for variance-covariance inequality, partitions error terms, and analyzes all voxels containing data. Group-level analyses were performed by entering the number of false alarms committed by

participants as a continuous covariate in a whole-brain regression. Monte Carlo simulation was used to compute a cluster threshold to correct for multiple comparisons using the updated (April, 2016) 3dFWHMx and 3dClustSim programs from the AFNI software package (Ward, 2000) and the group-level brain mask for analyses of interest. Simulations resulted in a voxel-wise threshold of p<.005 and a minimum cluster size of 173 voxels for the whole brain, corresponding to p<.05, Family-Wise Error (FWE) corrected.

Results

Behavioral Results

On average, participants successfully pressed on 95.0% of Go trials (*SD* = 5.51, *range* = 77–100%), and committed false alarms on 35.5% of Stop trials (*SD* = 5.63, *range* = 10–52%). On go trials, participants rarely committed direction errors (e.g., pressing with their right hand for a left-facing arrow; *M* = 1.24%, *SD* = 1.99, *range* = 0–12%; 67.2% of participants ≤ 1 direction error), and we counted these mismatch errors as incorrect Go trials. Stop signal reaction time (SSRT), or the rate of the Stop response, was 340 ms on average (*SD* = 45ms, *range* = 220–480ms). The number of false alarms was positively related to the number of successful go trials ($r = .29$, $p = .03$), as well as negatively related to the average reaction time (RT) on go trials ($r = -.76$; $p < .001$), suggesting that adolescents' false alarm rate was associated with the development of a stronger prepotent button press response. Furthermore, participants' total false alarm rate was, as expected, related to their SSRT ($r = .414$, $p = .002$). However, distinct from the total false alarm rate, SSRT was neither related to the number of successful go trials ($r = .187$, $p = .172$), nor the average RT on go trials ($r = .130$, $p = .343$).

fMRI Results

Effect of Accumulating False Alarm Errors on Neural Tracking—First, we examined the effect of accumulating FA errors on participants' neural tracking during go decisions. Adolescents showed positive tracking of accumulated false alarms in the dmPFC, mPFC, bilateral amygdala, bilateral hippocampus, and right temporal pole (Table 1; Figure 2). In other words, across the task, the more false alarms that adolescents committed, the greater these regions linearly increased in activation during go trials. The only area that showed negative tracking of accumulated errors was a region of the right inferior temporal cortex.

Associations between Neural Tracking of False Alarm Errors and Total False Alarms—Next, we examined individual differences in tracking of accumulating errors during go trials and the total number of false alarms adolescents committed. To this end, we entered the total false alarm rate as a regressor in a whole-brain regression analysis. Adolescents who showed reduced tracking of accumulating errors in the mPFC, dmPFC, OFC, bilateral IFG/AI, right temporal pole, and right intraparietal sulcus, showed greater average false alarm rates across the task (Table 2; Figure 3). This suggests that a lack of integration of error information into the ongoing task representation in these regions is associated with poorer task performance. Importantly, the mPFC region which showed an association with overall false alarm rate overlaps with the mPFC region that tracked

accumulating errors (Figure 4). Together, these two sets of findings indicate that while adolescents in general tend to track accumulating errors in the mPFC, those who show lower tracking in the mFPC commit greater overall errors across the task.

Competing Hypotheses—Finally, we performed two follow-up analyses in order to test the specificity of our effects. First, to ensure that results were not being driven by general inhibitory ability, we regressed SSRT on neural adaptation to accumulating FA errors on Go trials, which reveled significant effects in the medial OFC and thalamus. Secondly, we examined the relationship between neural adaptation to accumulating *successful* inhibition trials and the number of false alarm errors committed. We constructed a new model, where the parametric modulator instead tracked the accumulated number of successful inhibitions (as opposed to false alarms), and then entered total false alarms in a whole-brain regression analysis (see Table 1 for Main Effect). The right IFG/AI was the only region to show a significant relationship between tracking of successful inhibitions and the total false alarm rate. While some significant regions of activation emerged in these analyses, neither revealed activation in the mPFC (see Table 2 for both analyses), suggesting that neural adaptation in this region plays a particularly important role in tracking error commissions rather than tracking successes or general task ability.

Discussion

Previous examinations of learning and information integration processes have focused on learning in the context of explicit feedback based on task performance (e.g. van Duijvenvoorde et al., 2008; Peters et al., 2014). However, this approach does not capture the more-subtle ways in which individuals learn from and adjust their behavior in response to experience. We were specifically interested in the process of learning in the context of self-generated, error-related feedback. That is, how does internal recognition of errors, as well as subsequent neural integration of this error monitoring, relate to behavioral outcomes in task performance? Adolescence is a period of exploration and flexible adaptation to many new contexts and goals (Crone & Dahl, 2012), and integration of error-related information may help adolescents avoid repeating maladaptive behavioral strategies even when not receiving direct feedback from their environment. This internalized feedback learning mechanism may help adolescents evaluate their own behavior against previously learned rules without the need for continued external feedback. As such, examining the processes of this self-generated feedback learning can extend and complement findings using more-explicit feedback paradigms, giving us a more-complete understanding of the complex ways in which individuals learn.

Our findings suggest that adolescents show neural adaptation to the accumulation of false alarm errors across task performance. Specifically, when looking at go trials that follow increasing FA errors, adolescents show increased neural tracking in the mPFC, a region previously implicated in the integration of explicit feedback (van Duijvenvoorde et al., 2014; McCormick & Telzer, 2017b). This novel finding suggests that some of the same neural systems that support integration of explicit feedback (van Noordt & Segalowitz, 2012; van Duijvenvoorde et al., 2008; McCormick & Telzer, 2017b) are similarly involved in learning from self-generated, implicit feedback information. Adolescents also showed increased

tracking in the amygdala and hippocampus, structures involved in learning from negative information (Walker & Davis, 2002; Sigurdsson et al., 2007; Ruediger et al., 2012). Increased tracking in these regions may be related to detection of the error commission and the retrieval of goal-related information (i.e., that they should withhold a button press). Taken together, these findings suggest that as adolescents engage with the task, they maintain a neural trace of their prior performance. Excitingly, adolescents appear to do so even in the absence of instruction to keep track of errors, or any explicit indication of error commission within the task. Exhibition of this neural trace during go trials following accumulating errors likely reflects the role of these regions, and the mPFC in particular, in adjusting behavioral strategies to avoid future errors.

Importantly, an examination of individual differences in the neural tracking of accumulating errors revealed that individual differences in mPFC tracking was related to behavioral performance during the task. Adolescents who showed increased tracking of accumulating errors in the mPFC also showed lower overall false alarm rates across the task. This suggests that failing to integrate error-related feedback information results in higher commission of false alarm errors, while increased integration may help adolescents prevent future errors. Follow-up analyses support this inference, as mPFC tracking of FA errors was not related to general inhibitory ability, nor were the total number of false alarms committed by participants linked to mPFC tracking of successful inhibition trials, suggesting the particular importance of mPFC for tracking negative information about task performance. This is supported by previous research showing the importance of mPFC responsivity to negative, rather than positive, feedback as important for task behavior (McCormick & Telzer, 2017b).

The link between mPFC tracking of accumulating errors and total error rate may represent two potential forms of feedback-learning. One possibility might be that adolescents who show greater tracking are more sensitive to this form of self-generated, error-related feedback on an implicit level, and that increased tracking in the mPFC prompts behavioral changes that support avoidance of future errors. Alternatively, activation in the dmPFC, a region implicated in self-referential processing (see Northoff et al., 2006), might suggest that integration of error-related feedback involves self-evaluation of current behavioral strategies and how they might be changed in order to improve subsequent task performance. Disentangling whether this neural trace of error accumulation represents an automatic versus deliberative reaction to error commission should be a focus of future research. Furthermore, future research should investigate whether individual differences in mPFC tracking are stable, inter-individual trait differences in the reactivity of mPFC to negative feedback information, or whether these differences emerge *in vivo* during the task. The SST is not an ideal context to examine this question, as it adapts to changes in behavioral performance. Thus, future work should seek to disentangle behavioral and neural adaptation in response to error-related feedback.

These findings both support and extend previous research on feedback learning in important and novel ways. First, previous findings on feedback learning have involved explicit feedback (van Duijvenvoorde et al., 2014; McCormick & Telzer, 2017b), while the current study relied on internally-generated feedback in response to error commission. Additionally, these previous findings have been in the context of risk-taking behavior and rewards, while

the current study relies on a difficult behavioral inhibition task. However, despite these marked differences in context, the current findings support the idea that feedback-related processes may generalize across explicit and self-generated feedback types. Similar to mPFC recruitment following explicit negative feedback (McCormick & Telzer, 2017b), we find that the mPFC is involved in tracking the accumulation of errors. This points to a general role of the mPFC in integrating feedback information into on-going task representations, regardless of the source of that feedback. Furthermore, we found that decreased tracking of false alarm errors in the mPFC was related to poorer behavioral performance across the task, reflecting a "cool" counterpart to the increase in risk behavior seen in adolescents who show reduced mPFC activation following negative feedback in a risky context (McCormick & Telzer, 2017b). This exciting replication across samples and context may offer a potential answer to questions previously posed regarding whether mPFC reactivity in a risky context are the result of intrinsic sensitivity to negative feedback versus goal-directed suppression of sensitivity to feedback (McCormick & Telzer, 2017b). In contrast to risk-taking tasks where rewards can be obtained through risky behavior, there is no value to ignore feedback information in the SST. Indeed, the stated goal of the task is to avoid false alarm errors, reducing participants' motivation to ignore error-related feedback. These two findings, therefore, appear to argue for the view of mPFC reactivity to negative feedback (either external or internal) as reflecting an intrinsic difference in sensitivity to that negative information.

In conclusion, we took a novel approach by modeling neural activation changes across the SST in response to accumulating errors. In doing so, we offer the first evidence that individuals track behavioral inhibition performance in a region of the mPFC previously implicated in feedback integration (van Duijvenvoorde et al., 2014; McCormick & Telzer, 2017b). Furthermore, we found that individual differences in this tracking of errors in the mPFC is related to performance on the task. Excitingly, we found a negative relationship between mPFC tracking of errors and total false alarm error rate. While a positive relationship might suggest that those with greater errors simply have more data to boost signal in the mPFC, adolescents who showed the greatest mPFC tracking of accumulating errors showed that effect despite having the fewest false alarms overall. Taken together with previous work (McCormick & Telzer, 2017b), these findings suggest a domain-general role for the mPFC in the integration of feedback information. This correspondence across contexts offers an exciting new extension of our understanding of learning processes that do not rely on external, explicit feedback cues.

Acknowledgments

We greatly appreciate the assistance of the Biomedical Imaging Center at the University of Illinois, as well as Susannah Ivory, Kathy Do, Michael Perino, Heather Ross, Lynda Lin, and Tae-Ho Lee for assistance collecting data. This research was supported by grants from the National Institutes of Health (R01DA039923) and National Science Foundation (SES 1459719).

References

Crone EA, Dahl RE. Understanding adolescence as a period of social–affective engagement and goal flexibility. Nature Reviews Neuroscience. 2012; 13(9):636–650. [PubMed: 22903221]

Ernst M, Nelson EE, Jazbec S, McClure EB, Monk CS, Leibenluft E, Pine DS. Amygdala and nucleus accumbens in responses to receipt and omission of gains in adults and adolescents. NeuroImage. 2005; 25(4):1279–1291. [PubMed: 15850746]

Galvan A. The Teenage Brain Sensitivity to Rewards. Current Directions in Psychological Science. 2013; 22(2):88–93.

Gee DG, Humphreys KL, Flannery J, Goff B, Telzer EH, Shapiro M, Tottenham N. A developmental shift from positive to negative connectivity in human amygdala–prefrontal circuitry. The Journal of Neuroscience. 2013; 33(10):4584–4593. [PubMed: 23467374]

Logan GD, Cowan WB. On the ability to inhibit thought and action: A theory of an act of control. Psychological Review. 1984; 91(3):295.

McCormick EM, Telzer EH. Adaptive adolescent flexibility: Neurodevelopmental of decision-making and learning in a risky context. Journal of Cognitive Neuroscience. 2017a; 29:413–423. [PubMed: 28129057]

McCormick EM, Telzer EH. Failure to retreat: blunted sensitivity to negative feedback supports risky behavior in adolescents. NeuroImage. 2017b; 147:381–389. [PubMed: 27989774]

Mueller SC, Maheu FS, Dozier M, Peloso E, Mandell D, Leibenluft E, Ernst M. Early-life stress is associated with impairment in cognitive control in adolescence: an fMRI study. Neuropsychologia. 2010; 48(10):3037–3044. [PubMed: 20561537]

Northoff G, Heinzel A, De Greck M, Bermpohl F, Dobrowolny H, Panksepp J. Self-referential processing in our brain—a meta-analysis of imaging studies on the self. NeuroImage. 2006; 31(1): 440–457. [PubMed: 16466680]

Paus T. Mapping brain maturation and cognitive development during adolescence. Trends in Cognitive Sciences. 2005; 9(2):60–68. [PubMed: 15668098]

Peters S, Braams BR, Raijmakers ME, Koolschijn PCM, Crone EA. The neural coding of feedback learning across child and adolescent development. Journal of Cognitive Neuroscience. 2014; 26(8): 1705–1720. [PubMed: 24564463]

Peters S, Van Duijvenvoorde AC, Koolschijn PCM, Crone EA. Longitudinal development of frontoparietal activity during feedback learning: contributions of age, performance, working memory and cortical thickness. Developmental Cognitive Neuroscience. 2016; 19:211–222. [PubMed: 27104668]

Phelps EA, Delgado MR, Nearing KI, LeDoux JE. Extinction learning in humans: role of the amygdala and vmPFC. Neuron. 2004; 43(6):897–905. [PubMed: 15363399]

Rubia K, Smith AB, Brammer MJ, Taylor E. Right inferior prefrontal cortex mediates response inhibition while mesial prefrontal cortex is responsible for error detection. NeuroImage. 2003; 20(1):351–358. [PubMed: 14527595]

Ruediger S, Spirig D, Donato F, Caroni P. Goal-oriented searching mediated by ventral hippocampus early in trial-and-error learning. Nature Neuroscience. 2012; 15(11):1563–1571. [PubMed: 23001061]

Satterthwaite TD, Wolf DH, Loughead J, Ruparel K, Elliott MA, Hakonarson H, Gur RE. Impact of in-scanner head motion on multiple measures of functional connectivity: relevance for studies of neurodevelopment in youth. NeuroImage. 2012; 60(1):623–632. [PubMed: 22233733]

Schwarz AJ, Gozzi A, Reese T, Bifone A. In vivo mapping of functional connectivity in neurotransmitter systems using pharmacological MRI. NeuroImage. 2007; 34(4):1627–1636. [PubMed: 17188903]

Sigurdsson T, Doyere V, Cain CK, LeDoux JE. Long-term potentiation in the amygdala: a cellular mechanism of fear learning and memory. Neuropharmacology. 2007; 52(1):215–227. [PubMed: 16919687]

Somerville LH, Jones RM, Casey BJ. A time of change: behavioral and neural correlates of adolescent sensitivity to appetitive and aversive environmental cues. Brain and Cognition. 2010; 72(1):124–133. [PubMed: 19695759]

Stevens MC, Kiehl KA, Pearlson GD, Calhoun VD. Brain network dynamics during error commission. Human Brain Mapping. 2009; 30(1):24–37. [PubMed: 17979124]

Supekar K, Uddin LQ, Prater K, Amin H, Greicius MD, Menon V. Development of functional and structural connectivity within the default mode network in young children. NeuroImage. 2010; 52(1):290–301. [PubMed: 20385244]

Telzer EH. Dopaminergic reward sensitivity can promote adolescent health: A new perspective on the mechanism of ventral striatum activation. Developmental Cognitive Neuroscience. 2016; 17:57–67. [PubMed: 26708774]

Thakkar KN, Congdon E, Poldrack RA, Sabb FW, London ED, Cannon TD, Bilder RM. Women are more sensitive than men to prior trial events on the Stop-signal task. British Journal of Psychology. 2014; 105(2):254–272. [PubMed: 24754812]

Tohka J, Foerde K, Aron AR, Tom SM, Toga AW, Poldrack RA. Automatic independent component labeling for artifact removal in fMRI. NeuroImage. 2008; 39(3):1227–1245. [PubMed: 18042495]

van den Bos W, Cohen MX, Kahnt T, Crone EA. Striatum–medial prefrontal cortex connectivity predicts developmental changes in reinforcement learning. Cerebral Cortex. 2012; 22(6):1247–1255. [PubMed: 21817091]

van Duijvenvoorde AC, de Macks ZAO, Overgaauw S, Moor BG, Dahl RE, Crone EA. A cross-sectional and longitudinal analysis of reward-related brain activation: effects of age, pubertal stage, and reward sensitivity. Brain and Cognition. 2014; 89:3–14. [PubMed: 24512819]

van Duijvenvoorde AC, Zanolie K, Rombouts SA, Raijmakers ME, Crone EA. Evaluating the negative or valuing the positive? Neural mechanisms supporting feedback-based learning across development. The Journal of Neuroscience. 2008; 28(38):9495–9503. [PubMed: 18799681]

van Noordt SJ, Segalowitz SJ. Performance monitoring and the medial prefrontal cortex: a review of individual differences and context effects as a window on self-regulation. Frontiers in Human Neuroscience. 2012; 6:197. [PubMed: 22798949]

Verbruggen F, Logan GD. Response inhibition in the stop-signal paradigm. Trends in Cognitive Sciences. 2008; 12(11):418–424. [PubMed: 18799345]

Walker DL, Davis M. The role of amygdala glutamate receptors in fear learning, fear-potentiated startle, and extinction. Pharmacology Biochemistry and Behavior. 2002; 71(3):379–392.

Williams BR, Ponesse JS, Schachar RJ, Logan GD, Tannock R. Development of inhibitory control across the life span. Developmental Psychology. 1999; 35(1):205. [PubMed: 9923475]

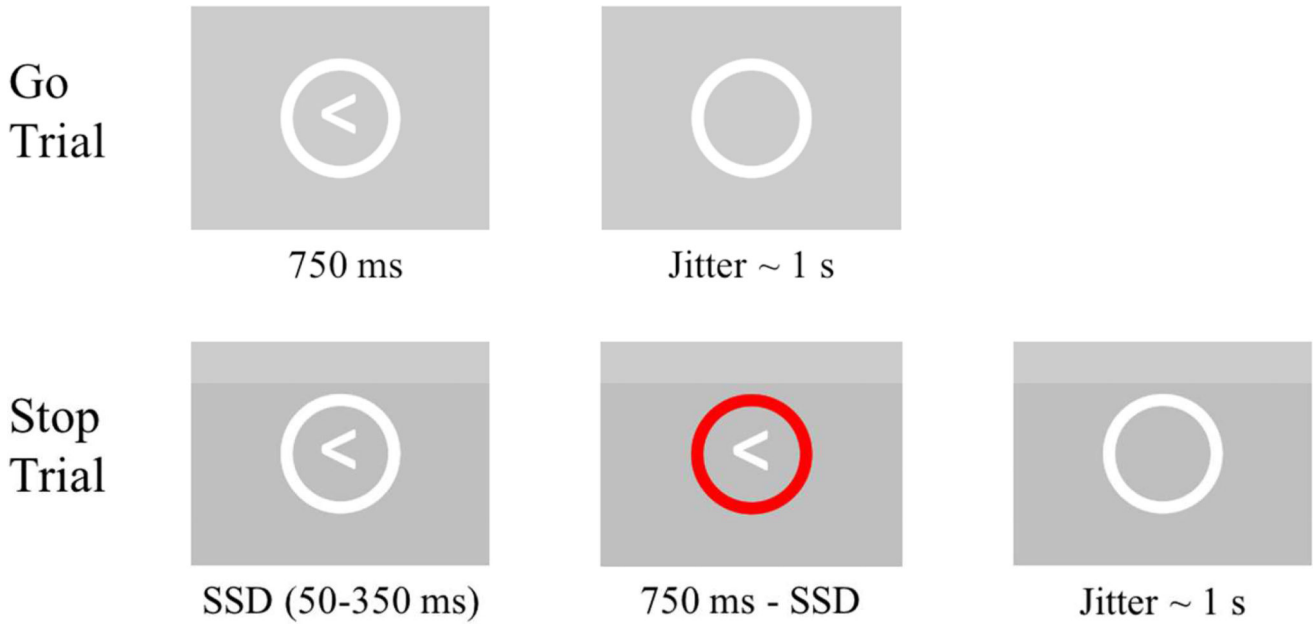

Figure 1.

On Go Trials (66.7% of trials), participants were instructed to execute a button press corresponding to the direction of the presented arrow. On Stop Trials (33.3% of trials), participants were instructed to withhold a button press if the circle turned red. The Stop Signal Delay (SSD; initial = 150 ms) was increased by 50 ms after each successful Stop trial and decreased by 50 ms after each unsuccessful Stop trial (i.e. false alarm).

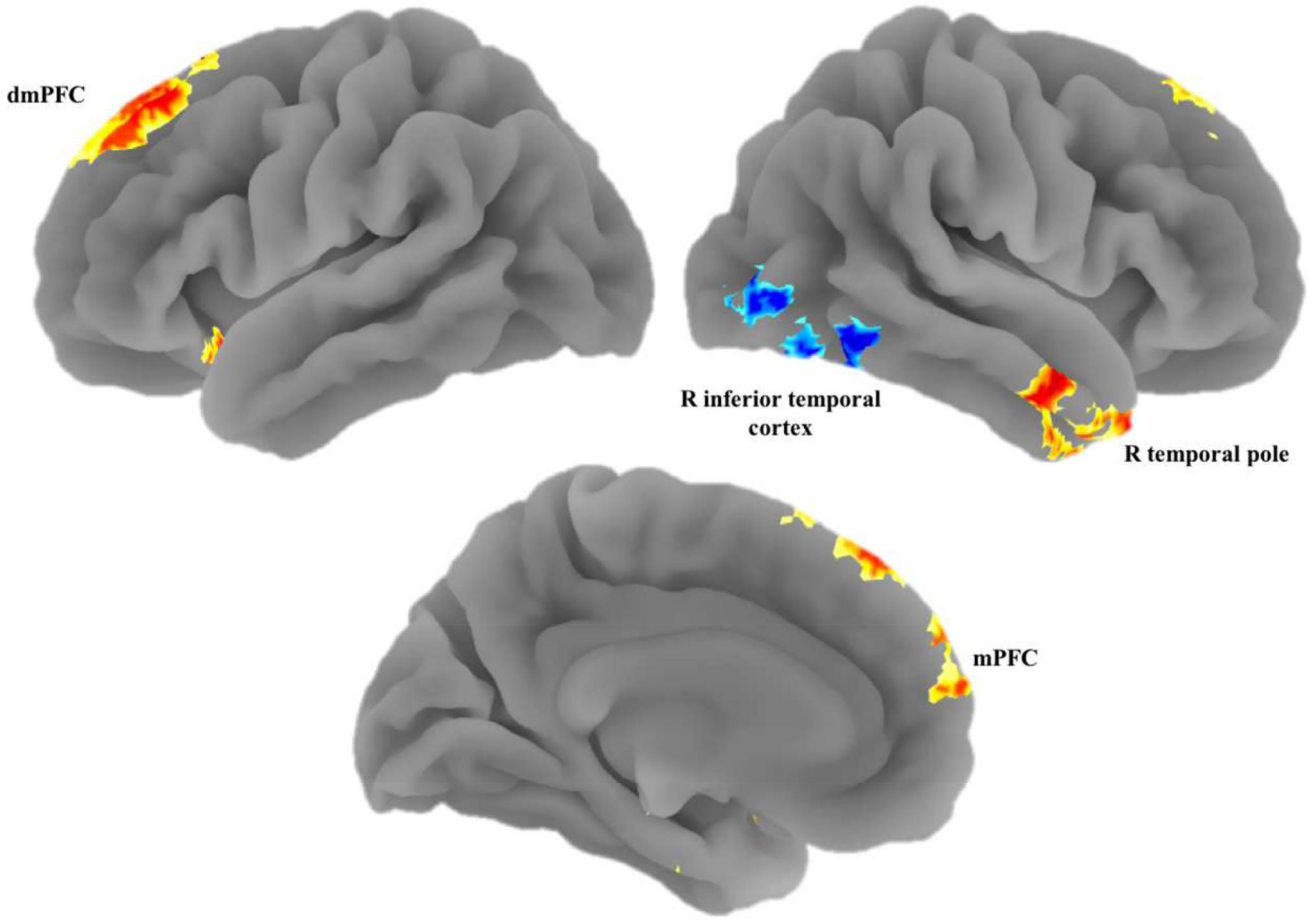

Figure 2.

We found increased tracking of accumulating false alarms during go trials in the mPFC, dmPFC, and right temporal pole, along with decreased tracking in the right inferior temporal cortex.

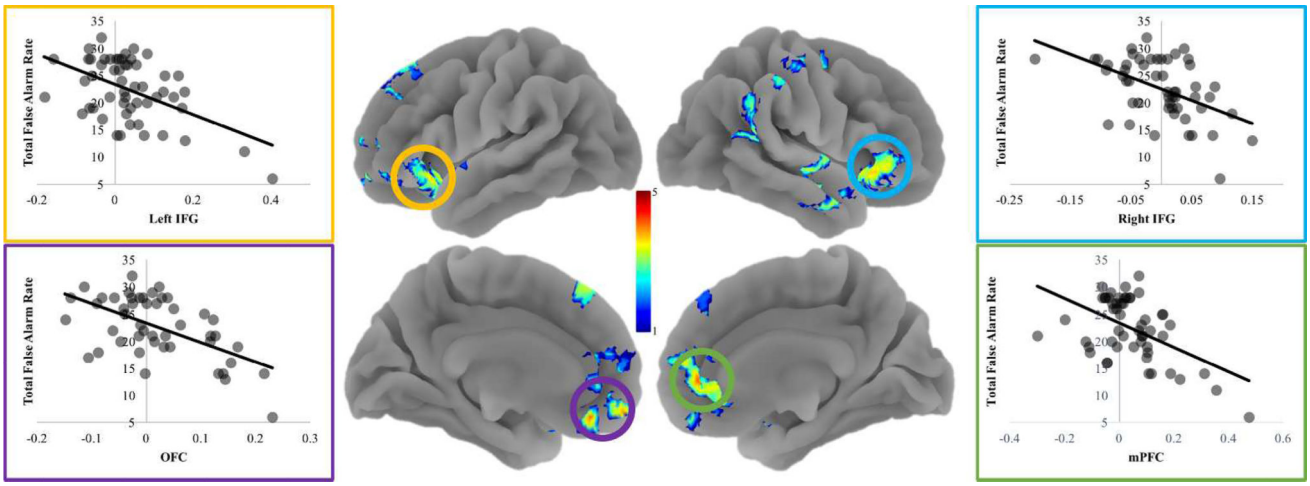

Figure 3.

We found that decreased tracking of accumulating false alarms in the mPFC, OFC, and bilateral IFG/AI was associated with fewer total false alarms.

Figure 4.
We created a mask of the voxels that showed overlap in the analyses tracking of error commission at the group level and those that showed decreased tracking when participants committed a greater number of false alarms. The overlap included k =229 voxels.

Table 1

Neural Regions Showing Significant Tracking of Accumulating False Alarm Errors or Successful Inhibitions During Go Trials

Anatomical Region	+/−	BA	x	y	z	t	k
Tracking of Accumulating Errors							
dmPFC[a]	+	9	−4	64	28	5.21	1596
mPFC[a]	+	8/9	−2	58	12	3.84	
R Temporal Pole[b]	+	38	52	−6	−30	4.50	1015
R Amygdala[b]	+		30	−2	−24	4.05	
R Hippocampus[b]	+		30	−10	−22	3.73	
L Hippocampus[c]	+		−26	−16	−20	4.35	462
L Amygdala[c]	+		−22	4	−20	3.71	
R ITG	−	20	44	−68	−22	4.64	813
Tracking of AccumulatingSuccessful Inhibitions							
dmPFC[d]	+	9	−6	62	26	4.86	1069
mPFC[d]	+	8/9	−2	62	16	4.42	
R Temporal Pole	+	38	34	4	−44	5.17	795
L Hippocampus	+		−32	−18	−20	4.37	294
Calcarine Gyrus	+	17	2	−82	14	5.16	850
R ITG	−	20	56	−54	−14	4.23	1604

Note: L and R refer to left and right hemispheres; + and − refer to positive or negative tracking; BA refers to Brodmann Area of peak voxel; k refers to the number of voxels in each significant cluster; t refers to peak activation level in each cluster; x, y, and z refer to MNI coordinates.

Superscripts (e.g. a, b, etc.) indicate that peak voxels are part of a contiguous cluster. dmPFC = Dorsomedial Prefrontal cortex; mPFC = Medial Prefrontal Cortex; IFG = Inferior Frontal Gyrus; ITG = Inferior Temporal Gyrus.

Table 2

Neural Regions Showing Significant Tracking of Accumulating False Alarm Errors during Go Trials and links with Task Behavior

Anatomical Region	+/−	BA	x	y	z	t	k
Tracking of Accumulating Errors							
Total False Alarms							
Medial OFC[a]	+	11	−4	40	−18	5.02	1879
mPFC[a]	+	8/9	0	48	6	4.27	
dmPFC	+	9	20	46	46	4.99	1003
R IFG/AI[b]	+	45	36	26	−8	4.44	1068
R Temporal Pole[b]	+	38	52	−12	−18	5.73	
L IFG/AI[c]	+	45	−32	26	−10	4.56	1315
IPS	+	7	52	−44	16	3.87	671
R Postcentral Gyrus	+	3	48	−20	54	3.38	249
SSRT							
Medial OFC	−	11	2	50	−20	3.98	274
Thalamus	−		−10	−12	14	3.59	179
Tracking of Accumulating Successful Inhibitions							
Total False Alarms							
R IFG/AI	−	45	36	28	−6	4.56	205

Note: L and R refer to left and right hemispheres; + and − refer to positive or negative tracking; BA refers to Brodmann Area of peak voxel; k refers to the number of voxels in each significant cluster; t refers to peak activation level in each cluster; x, y, and z refer to MNI coordinates.

Superscripts (e.g. a, b, etc.) indicate that peak voxels are part of a contiguous cluster. OFC = Orbitofrontal Cortex; mPFC = Medial Prefrontal Cortex; dmPFC = Dorsomedial Prefrontal cortex; IFG = Inferior Frontal Gyrus; AI = Anterior Insula; IPS = Inferior Parietal Sulcus.